JOURNAL OF GEOPHYSICAL RESEARCH, VOL. 99, NO. B7, PAGES 13,767–13,779, JULY 10, 1994

Dislocations in inhomogeneous media via a moduli perturbation approach: General formulation and two-dimensional solutions

Yijun Du
Department of Geological and Environmental Sciences, Stanford University, Stanford, California

Paul Segall
Department of Geophysics, Stanford University, Stanford, California

Huajian Gao
Division of Applied Mechanics, Stanford University, Stanford, California

Abstract. Quasi-static elastic dislocations in a homogeneous elastic half-space are commonly used to model earthquake faulting processes. Recent studies of the 1989 Kalapana, Hawaii, and Loma Prieta, California, earthquakes suggest that spatial variations in elastic properties are necessary to reconcile geodetic and seismic results (Arnadottir et al., 1991; Eberhart-Phillips and Stuart, 1992). In this paper, we use a moduli perturbation approach to investigate the effect of lateral and vertical variations in elastic properties on the elastic fields produced by dislocations. The method is simple, efficient, and in some cases leads to closed form solutions. The zero-order solution is simply the solution for a homogeneous body. The first-order correction for elastic heterogeneity is given by a volume integral involving the spatial variations in moduli, the displacements due to a dislocation in a homogeneous half-space, and the half-space Green's function. The same representation can be also used to obtain higher-order solutions. If there are only piecewise constant variations in shear modulus, the volume integral can be reduced to a surface integral (or line integral in two-dimensions). Comparisons with the analytical solutions for a screw dislocation in a layered medium suggest that the perturbation solutions are valid for nearly an order of magnitude variation in modulus. It is shown that a simple two-dimensional model with both vertical and lateral variations in the elastic properties may explain a large part of the discrepancy between seismic and geodetically inferred fault depths for the 1989 Kalapana, Hawaii, earthquake.

Introduction

Following the pioneering work of *Steketee* [1958] and *Chinnery* [1961], numerous workers have used elastic dislocation theory to model earthquake faulting processes. More recently, several investigators have used standard inverse techniques in combination with elastic dislocations in a homogeneous, isotropic, half-space to solve for the distribution of slip (or slip rate) on a fault from crustal deformation data [e.g., *Segall and Harris*, 1986; *Ward and Barrientos*, 1986; *Du et al.*, 1992]. However, studies of two earthquakes that occurred in 1989, the Kalapana earthquake on the south flank of Kilauea volcano and the Loma Prieta earthquake in the Santa Cruz Mountains, have suggested that there are significant shortcomings in homogeneous elastic models [*Arnadottir et al.*, 1991; *Eberhart-Phillips and Stuart*, 1992]. Geodetically derived fault models of the 1989 Loma Prieta earthquake presented by *Lisowski et al.* [1990] and *Marshall et al.* [1991] are significantly different from the fault plane inferred from aftershock locations. *Eberhart-Phillips and Stuart* [1992] suggested that material contrasts across the fault could explain the discrepancy. *Arnadottir et al.* [1992] found that accounting for the correlations in the leveling data resolved the first-order discrepancy between the geodetic and seismic fault models. Analysis of the full geodetic data set shows that while there is not a significant discrepancy, the best fitting dislocation surface is biased toward the hanging wall side of the aftershock zone [*Arnadottir and Segall, 1994*]; this effect may be due to material heterogeneity. In their study of the 1989 Kalapana earthquake, *Arnadottir et al.* [1991] found that the fault depth inferred from leveling data, assuming a dislocation in a homogeneous half-space, was significantly shallower than that inferred from seismic data. The correlations in the leveling data were accounted for in this study. Finite element calculations suggested that elastic heterogeneity could explain a significant part, if not all, of the discrepancy [*Arnadottir et al.*, 1991]. We conclude that the widely used homogeneous elastic half space models may no longer be adequate to interpret the highly accurate geodetic data that are presently being collected.

In this paper, we investigate the effect of inhomogeneities on the elastic fields produced by a dislocation, and we develop an efficient method to compute the slip Green's function in inhomogeneous media for crustal deformation modeling. While numerous solutions exist in the literature for dislocations in special inhomogeneous media [e.g., *Weeks et al.*, 1968; *Rybicki*, 1971; *Barnett*, 1972; *Lee and Dundurs*, 1973; *Rybicki and*

Paper number 94JB00339.
0148-0227/94/94JB-00339$05.00

Kasahara, 1977; *Mahrer and Nur*, 1979; *Savage*, 1987; *Roth*, 1990], general solutions are difficult to obtain. On the other hand, one can use fully numerical methods, such as finite element or boundary element, to solve these problems. The difficulty is, of course, computational efficiency. It is relatively costly to carry out a three-dimensional (3-D) finite element or boundary element analysis, especially when the material properties vary rapidly at short spatial wavelengths. In this study, we use a linear moduli perturbation approach. The method is very general, simple to evaluate, and in some cases leads to closed form solutions.

First-order perturbation methods have already been used to find the effect of irregular surface topography on surface displacement fields [*McTigue and Stein*, 1984; *Meertens and Wahr*, 1986; *McTigue and Segall*, 1988]. *Gao* [1991] recently provided a systematic formulation of fracture analysis of inhomogeneous materials via the moduli perturbation approach and emphasized the calculations of the stress intensity factor at the crack tip in an inhomogeneous elastic medium. *Gao et al.* [1992] adopted the same moduli perturbation approach to construct a first-order solution for microindentation of thin films, and they found that the first-order perturbation solution is accurate up to a modulus contrast of a factor of 2. *Fan et al.* [1992] reformulated the moduli perturbation approach and showed that the inhomogeneity problem is converted to a series of inclusion problems using the eigenstrain concept. A similar technique was also used by *Walpole* [1967] to treat an inclusion in an anisotropic medium.

In the moduli perturbation procedure, a reference state, usually a homogeneous medium, is chosen to obtain the zeroth-order solution. It is shown that the first-order correction to the displacements can be represented by a volume integral in terms of the variations in moduli, the zeroth-order solution, and the displacement Green's function in the reference state. The same representation can be also used to iterate for higher-order solutions. The volume integral can be reduced to a surface integral (line integral in two dimensions) if there are only piecewise constant variations in shear modulus (layers, for example). Although in theory the variations in elastic properties should be small in order for the moduli perturbation method to work, comparisons with analytical solutions for a screw dislocation in a layered medium indicate that the perturbation results are valid over a substantial range of variations in moduli.

General Formulation of Moduli Perturbation Approach

We consider an elastic medium D bounded by a surface S containing a subdomain Ω surrounded by a surface Γ (Figure 1). S_t denotes the part of the surface S with the applied traction T_i, and S_u denotes the part of S with the prescribed displacement U_i. The stress σ_{ij} is given in terms of the displacement field u_i as

$$\sigma_{ij} = C_{ijkl}\, u_{k,l} \tag{1}$$

where subscripts to the right of the comma denote differentiation with respect to spatial coordinate, C_{ijkl} is the fourth-order elasticity tensor, and subscripts i, j, k, and l range over the Cartesian coordinates x, y, z. Assuming the elastic body is in equilibrium with body force $f(\mathbf{x})$ and some given boundary conditions, then the equations of equilibrium for the elastic system read

$$C_{ijkl}\, u_{k,lj} + u_{k,l}\, C_{ijkl,j} + f_i = 0 \tag{2}$$

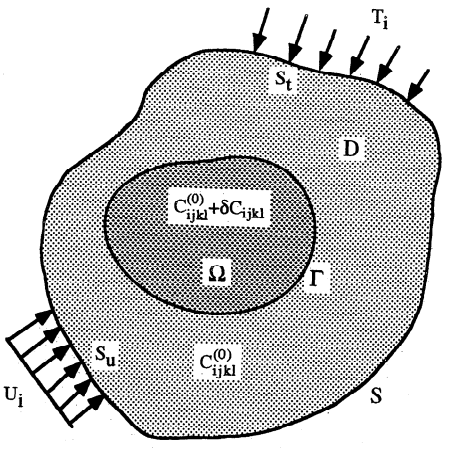

Figure 1. Geometrical configuration of an elastic inhomogeneous medium. The elastic medium is bounded by a surface S containing a subdomain Ω with variable modulus surrounded by a surface Γ. S_t denotes the part of S with the applied traction T_i, and S_u denotes the part of S with the prescribed displacement U_i. $C^{(0)}_{ijkl}$ is the fourth-order elasticity tensor for the domain D, and $C^{(0)}_{ijkl} + \delta C_{ijkl}(x)$ for the domain Ω.

with boundary conditions

$$\sigma_{ij}\, n_j = T_i \qquad \text{on} \qquad S_t \tag{3}$$

and

$$u_i = U_i \qquad \text{on} \qquad S_u. \tag{4}$$

The perturbation expansion is as follows. Let the moduli be a function of position $\mathbf{x}$ such that $C_{ijkl}(\mathbf{x})$ consist of some uniform part $C^{(0)}_{ijkl}$ plus a spatially varying perturbation $\delta C_{ijkl}(\mathbf{x})$ as

$$C_{ijkl}(\mathbf{x}) = C^{(0)}_{ijkl} + \delta C_{ijkl}(\mathbf{x}). \tag{5}$$

The displacement is expanded in a series as

$$u_i(\mathbf{x}) = u_i^{(0)}(\mathbf{x}) + u_i^{(1)}(\mathbf{x}) + u_i^{(2)}(\mathbf{x}) + \cdots + u_i^{(n)}(\mathbf{x}) + \cdots. \tag{6}$$

Substituting (5) and (6) into the governing equations and boundary conditions and collecting terms of like order, one obtains the following system of equations,

Zeroth order:

$$C^{(0)}_{ijkl}\, u^{(0)}_{k,lj} + f_i = 0 \tag{7a}$$

$$C^{(0)}_{ijkl}\, u^{(0)}_{k,l}\, n_j = T_i \qquad \text{on} \qquad S_t \tag{7b}$$

$$u_i^{(0)} = U_i \qquad \text{on} \qquad S_u \tag{7c}$$

First order:

$$C^{(0)}_{ijkl}\, u^{(1)}_{k,lj} + (\delta C_{ijkl}\, u^{(0)}_{k,l})_{,j} = 0 \tag{8a}$$

$$C^{(0)}_{ijkl}\, u^{(1)}_{k,l}\, n_j + \delta C_{ijkl}\, u^{(0)}_{k,l}\, n_j = 0 \qquad \text{on} \qquad S_t \tag{8b}$$

$$u_i^{(1)} = 0 \qquad \text{on} \qquad S_u \tag{8c}$$

Second order:

$$C^{(0)}_{ijkl}\, u^{(2)}_{k,lj} + (\delta C_{ijkl} u^{(1)}_{k,l})_{,j} = 0 \tag{9a}$$

$$C^{(0)}_{ijkl}\, u^{(2)}_{k,l}\, n_j + \delta C_{ijkl}\, u^{(1)}_{k,l}\, n_j = 0 \quad \text{on} \quad S_t \tag{9b}$$

$$u^{(2)}_i = 0 \quad \text{on} \quad S_u \tag{9c}$$

nth order:

$$C^{(0)}_{ijkl}\, u^{(n)}_{k,lj} + (\delta C_{ijkl} u^{(n-1)}_{k,l})_{,j} = 0 \tag{10a}$$

$$C^{(0)}_{ijkl}\, u^{(n)}_{k,l}\, n_j + \delta C_{ijkl}\, u^{(n-1)}_{k,l}\, n_j = 0 \quad \text{on} \quad S_t \tag{10b}$$

$$u^{(n)}_i = 0 \quad \text{on} \quad S_u. \tag{10c}$$

The zeroth-order problem is just the problem for a homogeneous medium $C^{(0)}_{ijkl}$. In the perturbation procedure, the zeroth-order solution $u^{(0)}_m$ is assumed to be known and is taken as a reference state for the perturbation. Note that for the first-order correction, the second terms in (8a) and (8b) are known from the specified variation in moduli and the solution to the zeroth-order problem. The inhomogeneous term in (8a) enters the equilibrium equations analogous to a known body force. Similarly, the inhomogeneous term in the boundary condition enters as a known distributed surface traction.

Let $G_{mi}(\mathbf{x},\mathbf{x}')$ be the elastic Green's function in a homogeneous medium, giving the displacement in the x_m direction at point $\mathbf{x}$ when the unit point force is acting in the direction x_i at $\mathbf{x}'$. Then the displacement due to distributed body forces $F_i(\mathbf{x})$ is given by $u_m(\mathbf{x}) = \int_v F_i(\mathbf{x}')G_{mi}(\mathbf{x},\mathbf{x}')dv(\mathbf{x}')$. Identifying the second term in (8a) as an equivalent body force and the second term in (8b) as an equivalent traction, we can write the solution to the first-order problem as

$$u^{(1)}_m(\mathbf{x}) = \int_D (\delta C_{ijkl}(\mathbf{x}')\, u^{(0)}_{k,l}(\mathbf{x}'))_{,j}\, G_{mi}(\mathbf{x},\mathbf{x}')dv(\mathbf{x}') - \int_S \delta C_{ijkl}(\mathbf{x}')\, u^{(0)}_{k,l}(\mathbf{x}')\, n_j\, G_{mi}(\mathbf{x},\mathbf{x}')ds(\mathbf{x}') \tag{11}$$

Application of the divergence theorem and chain rule allow equation (11) to be reduced to a single volume integral in terms of the variation in moduli, the zeroth-order solution, and the displacement Green's function for the reference state

$$u^{(1)}_m(\mathbf{x}) = -\int_\Omega \delta C_{ijkl}(\mathbf{x}')\, u^{(0)}_{k,l}(\mathbf{x}')\, G_{mi,j}(\mathbf{x},\mathbf{x}')\, dv(\mathbf{x}'). \tag{12}$$

The domain of integration is Ω, since $\delta C_{ijkl} = 0$ outside Ω. Similarly, for the second-order problem, the solution is obtained as

$$u^{(2)}_m(\mathbf{x}) = -\int_\Omega \delta C_{ijkl}(\mathbf{x}')\, u^{(1)}_{k,l}(\mathbf{x}')\, G_{mi,j}(\mathbf{x},\mathbf{x}')\, dv(\mathbf{x}'). \tag{13}$$

In general, the nth-order solution is expressed in terms of the proceeding lower-order solution as

$$u^{(n)}_m(\mathbf{x}) = -\int_\Omega \delta C_{ijkl}(\mathbf{x}')\, u^{(n-1)}_{k,l}(\mathbf{x}')\, G_{mi,j}(\mathbf{x},\mathbf{x}')\, dv(\mathbf{x}'). \tag{14}$$

We note that the first-order solution is similar to the Born approximation in elastodynamics [*Aki and Richards*, 1980] and that higher-order solutions are equivalent to the higher-order Born approximation [*Hudson and Heritage*, 1981].

For an isotropic medium, the variation in moduli can be written as

$$\delta C_{ijkl} = \frac{2\mu_\Omega \delta\nu}{(1-2\nu_\Omega)(1-2\nu_0)}\delta_{ij}\delta_{kl} + \frac{\delta\mu}{\mu_0}C^{(0)}_{ijkl} \tag{15}$$

where μ_0 and ν_0 are the shear modulus and Poisson's ratio for the reference body respectively, μ_Ω and ν_Ω are the shear modulus and Poisson's ratio for the inhomogeneous region, $\delta\nu = \nu_\Omega - \nu_0$, $\mu = \mu_\Omega - \mu_0$, and δ_{ij} is the Kronecker delta. Therefore, for variations only in Poisson's ratio, the volume integral in (14) is with respect to the dilatational component of the source field, which is often easier to evaluate. If there are only piecewise constant variations in shear modulus (layers, for example), then the volume integral of (14) can be reduced to a surface integral (line integral in two dimensions) using the divergence theorem

$$u^{(n)}_m(\mathbf{x}) = -\frac{\delta\mu}{\mu_0}\int_\Gamma \sigma^{(n-1)}_{ij}(\mathbf{x}')\, G_{mi}(\mathbf{x},\mathbf{x}')\, n_j\, ds(\mathbf{x}') \tag{16a}$$

where

$$\sigma^{(n-1)}_{ij} = C^{(0)}_{ijkl}\, u^{(n-1)}_{k,l}. \tag{16b}$$

Here we have made use of the fact that from (7) - (10), $\sigma^{(n-1)}_{ij,j} = 0$. From (16) it is apparent that the correction at nth order is proportional to $(\delta\mu/\mu_0)^n$. Therefore to guarantee the convergence of the perturbation expansion, a reference state should be chosen so that $\delta\mu/\mu_0$ is less than 1.

It should be pointed out that other problems with known solutions can be chosen as a reference state (not necessarily homogeneous). However, a proper reference state should be chosen so that the imposed perturbation does not change the nature of the original problem. For example, the singularity at an interface crack tip cannot be derived from a zero-order solution in a homogeneous space [*Gao*, 1991]. The singularity at the interface crack tip is a special characteristic of the original problem which must appear in the zero-order solution.

To test the perturbation method, we consider an antiplane problem with a vertical finite dislocation in a semi-infinite layered medium in the next section.

A Screw Dislocation in a Two-Dimensional Semi-Infinite Layered Medium

A Screw Dislocation in Substrate

Consider a two-dimensional (2-D) semi-infinite, elastic, isotropic medium with a coordinate system chosen as in Figure 2a. The surface layer has a thickness of H with a shear modulus of μ_1, and the substrate has an infinite extension downward with a shear modulus of μ_2. A finite vertical screw dislocation is located from depth d to D in the lower layer. Since the model is antiplane, the displacements are only in the x_1 direction and depend only on x_2 and x_3. The displacement discontinuity across the dislocation surface, i.e., the magnitude of the Burger's vector, is b. This problem has been solved by *Rybicki* [1971] using an image method, where the solution is in the form of an infinite series. In the following, we will present a moduli perturbation solution.

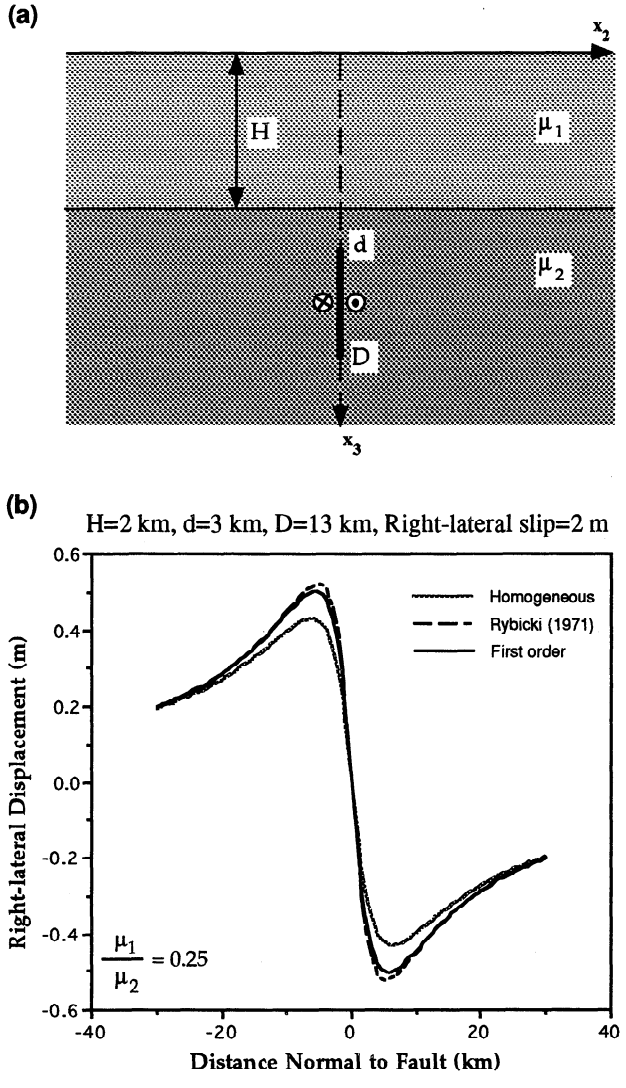

Figure 2. (a) A finite screw dislocation at depths of d to D in a layered semi-infinite medium. (b) Comparison of first-order perturbation solution with that obtained by *Rybicki* [1971] using an image method and with that for homogeneous medium for a screw dislocation buried in the substrate.

Following *Muskhelishvilli* [1953], a complex potential $\omega(z)$ can be used to represent the antiplane displacement and stress components in a homogeneous body as

$$u_1 = \frac{1}{\mu}\mathrm{Im}[\omega(z)] \tag{17a}$$

$$\sigma_{13} = \mathrm{Re}[\omega'(z)] \tag{17b}$$

where $z = x_2 + ix_3$, and $\mathrm{Re}[F]$ and $\mathrm{Im}[F]$ denote the real and imaginary parts of the complex quantity, and $\omega'(z)$ is the derivative of the complex potential $\omega(z)$. For a screw dislocation located at depth of d on the x_3 axis in a homogeneous half-plane, the complex potential $\omega(z)$ is given by

$$\omega(z) = \frac{\mu b}{2\pi}[\ln(z-id) - \ln(z+id)] \tag{18}$$

The solution for a screw dislocation in a finite interval $[d, D]$ can be obtained by adding a oppositely signed dislocation at depth D. The displacement Green's function for the homogeneous half-plane is expressed as

$$G_{11} = \frac{1}{2\pi\mu}\{Re[\ln(z+z')] - Re[\ln(z-z')]\} \tag{19}$$

The zeroth-order solution at the free surface (for simplicity, only the expressions at the free surface are given in the text below; see Appendix A for the full expressions) is given as

$$u_1^{(0)} = \frac{b}{\pi}[\tan^{-1}(\frac{x_2}{d}) - \tan^{-1}(\frac{x_2}{D})]. \tag{20}$$

The first- and second-order corrections are

$$u_1^{(1)}(x_2, 0) = -\frac{\delta\mu}{\mu_2}\int_{-\infty}^{+\infty} \sigma_{13}^{(0)}(x_2', H)\, G_{11}[(x_2, 0), (x_2', H)]\, dx_2' \tag{21}$$

$$u_1^{(2)}(x_2, 0) = -\frac{\delta\mu}{\mu_2}\int_{-\infty}^{+\infty} \sigma_{13}^{(1)}(x_2', H)\, G_{11}[(x_2, 0), (x_2', H)]\, dx_2' \tag{22}$$

where $\delta\mu = \mu_1 - \mu_2$, and $\sigma_{13}^{(1)} = \mu_2 u_{1,3}^{(0)}$. After some mathematical manipulations, the first- and second-order displacement corrections at the free surface are obtained as

$$u_1^{(1)} = \frac{(1-\gamma)b}{2\pi}[\tan^{-1}(\frac{x_2}{d}) - \tan^{-1}(\frac{x_2}{D}) - \tan^{-1}(\frac{x_2}{d+2H}) + \tan^{-1}(\frac{x_2}{D+2H})] \tag{23}$$

$$u_1^{(2)} = \frac{(1-\gamma)^2 b}{4\pi}[\tan^{-1}(\frac{x_2}{d}) - \tan^{-1}(\frac{x_2}{D}) - 2\tan^{-1}(\frac{x_2}{d+2H}) + 2\tan^{-1}(\frac{x_2}{D+2H}) + \tan^{-1}(\frac{x_2}{d+4H}) - \tan^{-1}(\frac{x_2}{D+4H})], \tag{24}$$

where $\gamma = \mu_1/\mu_2$. The Shanks transformation can be used to improve the estimate of the sum of a series [*Bender and Orszag*, 1978]. By applying a Shanks transformation to the second-order solution, we can obtain an improved estimate of the surface displacement as

$$u_1 = \frac{u_1^{(1)}[u_1^{(0)} + u_1^{(1)}] - u_1^{(0)}u_1^{(2)}}{u_1^{(1)} - u_1^{(2)}} \tag{25}$$

which is accurate to third order. For simplicity, we refer to the Shanks transformation of the second-order solution as a third-order solution.

In Figure 2b, we compare the first-order perturbation solution with Rybicki's solution and with the solution for a homogeneous medium for $\gamma = 0.25$, $H = 2$ km, $d = 3$ km, $D = 13$ km, and right-lateral slip of 2 m. It is shown that a softer surface layer amplifies the surface displacement significantly and that the first-order solution agrees well with Rybicki's solution. In the following, we will make a detailed comparison between the perturbation and Rybicki's solutions.

The errors between the first-order and Rybicki's solutions for various values of γ are shown in Figure 3. The maximum error decreases with decreasing shear modulus contrast from 8.7% for $\gamma = 0.1$ to 0.5% for $\gamma = 0.75$. If we go to higher-order solutions, then the error can be made arbitrarily small. In Figure 4 we compare the errors between various orders of perturbation solutions and Rybicki's image solution for a shear modulus contrast of 4 times ($\gamma = 0.25$). The maximum error is as much as 23% for no correction (zeroth-order solution) but decreases

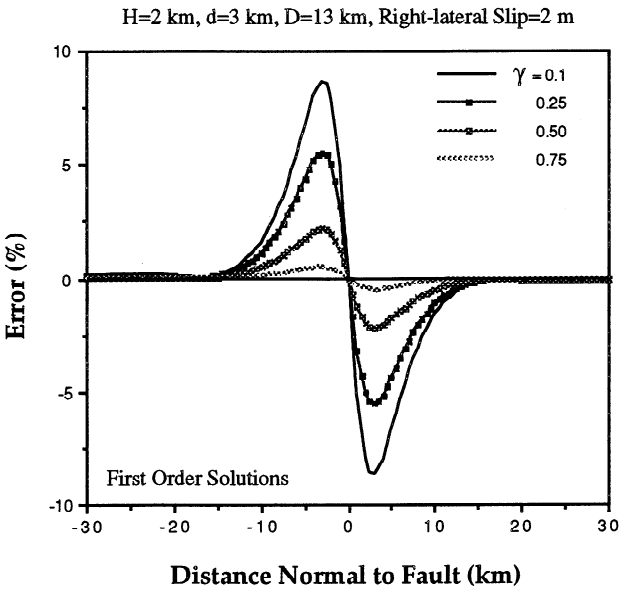

Figure 3. Percent error (= $|u_{Rybicki}-u_p|/\max|u_{Rybicki}|$) in first-order perturbation solution as a function of distance normal to fault.

rapidly to less than ~6% with a first-order correction and to less than 2% with a second-order correction. The error is less than 0.2% for third order solution. The first-order correction is most significant, and the errors for the first-order solutions are less than 10% even for a factor of 10 contrast in shear modulus.

A Screw Dislocation in Surface Layer

As a further test of the perturbation approach, we consider a finite screw dislocation within the surface layer. Assuming that the dislocation reaches the surface, i.e., $d = 0$, $0 < D \leq H$ (see Figure 2a for geometry), then the zeroth-order solution and first-order and second-order surface displacement corrections are given as

$$u_1^{(0)} = \frac{b}{\pi}\tan^{-1}\left(\frac{D}{x_2}\right) \tag{26}$$

$$u_1^{(1)} = \frac{(1-\gamma)b}{2\pi}\left[\tan^{-1}\left(\frac{x_2}{D-2H}\right) + \tan^{-1}\left(\frac{x_2}{D+2H}\right)\right] \tag{27}$$

$$u_1^{(2)} = \frac{(1-\gamma)^2 b}{4\pi}\left[\tan^{-1}\left(\frac{x_2}{D+2H}\right) + \tan^{-1}\left(\frac{x_2}{D-2H}\right) - \tan^{-1}\left(\frac{x_2}{D+4H}\right) - \tan^{-1}\left(\frac{x_2}{D-4H}\right)\right] \tag{28}$$

Figure 5 shows the comparison of surface displacements between first-order perturbation and Rybicki solutions for a shear modulus ratio of 0.25. The thickness of the surface layer is 5 km and the vertical screw dislocation lies at depths of 0 - 4 km and has a right-lateral slip of 2 m. The plot shows that the surface strain is more concentrated due to the presence of the softer surface layer and that the first-order perturbation solution agrees well with that of *Rybicki* [1971].

Figure 6 shows the error between first-order and Rybicki's solutions for various values of γ. The maximum error decreases with decreasing shear modulus contrast from ~25% for $\gamma = 0.1$ to ~1% for $\gamma = 0.75$. Higher-order solutions make the error much smaller. In Figure 7 we compare the error between various orders of perturbation solutions and Rybicki's image solution for a fixed shear modulus contrast of 4 ($\gamma = 0.25$). It is shown that the error is as much as 50% with no correction (zeroth-order solution) and decreases rapidly to ~13.5% with a first-order correction and to ~4% with a second-order correction. Thus these results confirm the conclusion of preceding section that the first-order correction is the most significant. The errors for the first-order solutions are less than 14% for a factor of 4 contrast in shear modulus if the screw dislocation is situated in the surface layer.

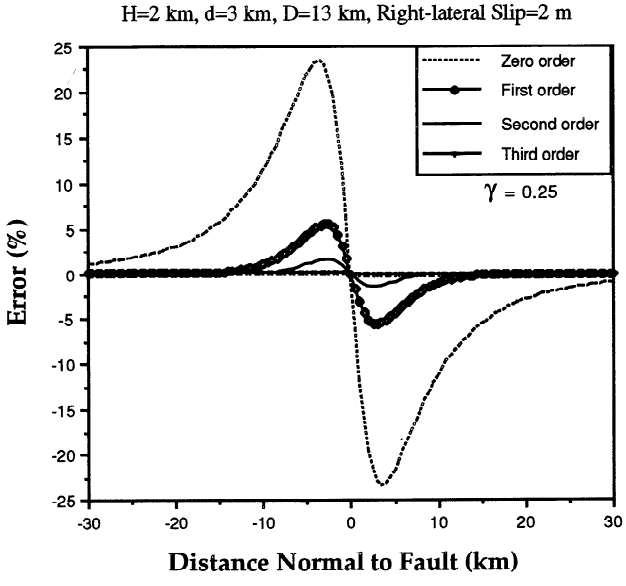

Figure 4. Percent error (= $|u_{Rybicki}-u_p|/\max|u_{Rybicki}|$) in various order perturbation solutions as a function of distance normal to fault.

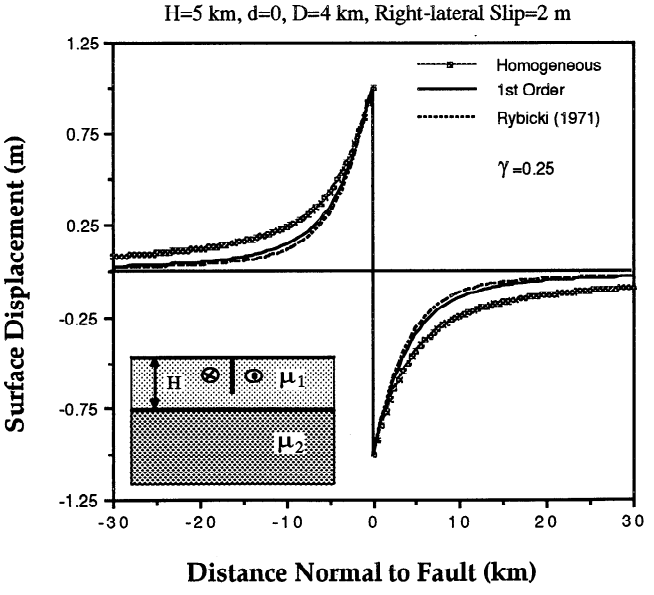

Figure 5. Surface displacements due to a dislocation in surface layer as a function of distance normal to fault for first-order perturbation and Rybicki solutions and that for homogeneous medium.

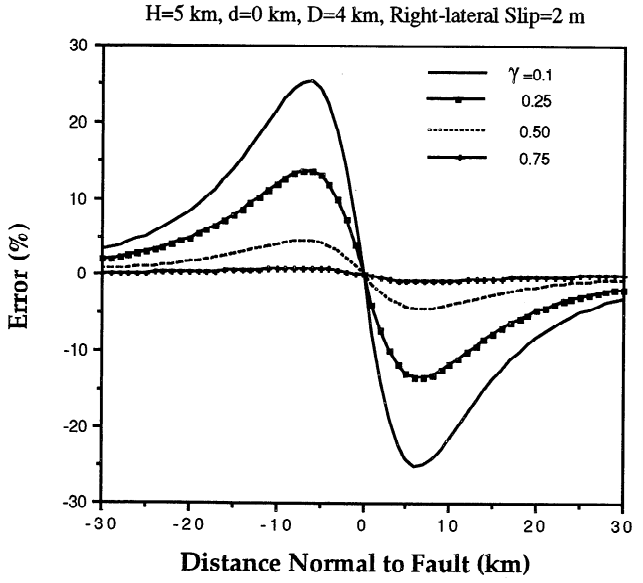

Figure 6. Percent error (= $|u_{Rybicki}-u_p|/\max|u_{Rybicki}|$) in first-order perturbation solution as a function of distance normal to fault.

Edge Dislocations in 2-D Semi-infinite Inhomogeneous Media

In this section, we consider an edge dislocation in 2-D semi-infinite inhomo-geneous media. We assume that there are only piecewise constant variations in shear modulus, and only first-order perturbation solutions will be presented using (16). The displacement Green's functions for the semi-infinite homo-geneous medium corresponding to a point force have been given by *Maruyama* [1966] (see Appendix B). The expressions for stresses due to an edge dislocation in a homogeneous semi-infinite medium have been given by *Head* [1953] (Appendix C).

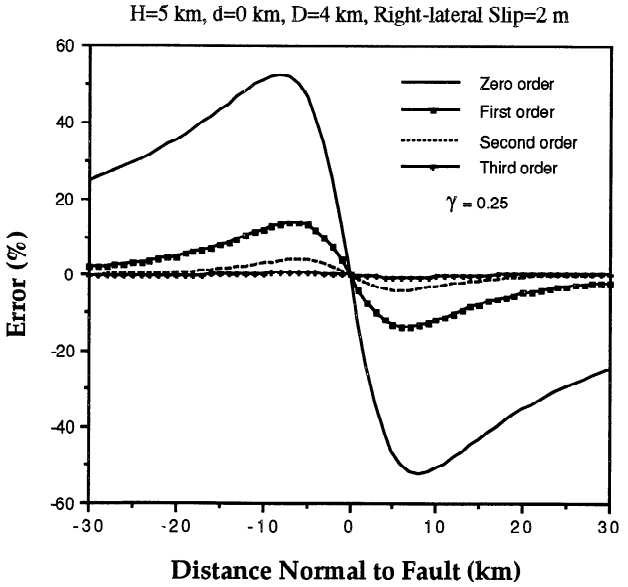

Figure 7. Percent error (= $|u_{Rybicki}-u_p|/\max|u_{Rybicki}|$) in various order perturbation solutions as a function of distance normal to fault.

The displacements in a homogeneous half-space due to an edge dislocation can be derived from *Mura* [1968] (Appendix D). The integral in (16a) is numerically evaluated using Romberg's integration method [*Press et al.*, 1986].

A Vertical Edge Dislocation in a Semi-infinite Horizontally Layered Medium

As an example, we first consider a vertical edge dislocation in a horizontally layered medium (Figure 8b insert). The parameter γ again denotes the ratio of the shear modulus for surface layer, μ_1, over the shear modulus for the substrate, μ_2. The thickness of the surface layer is 5 km, and the top of the vertical edge

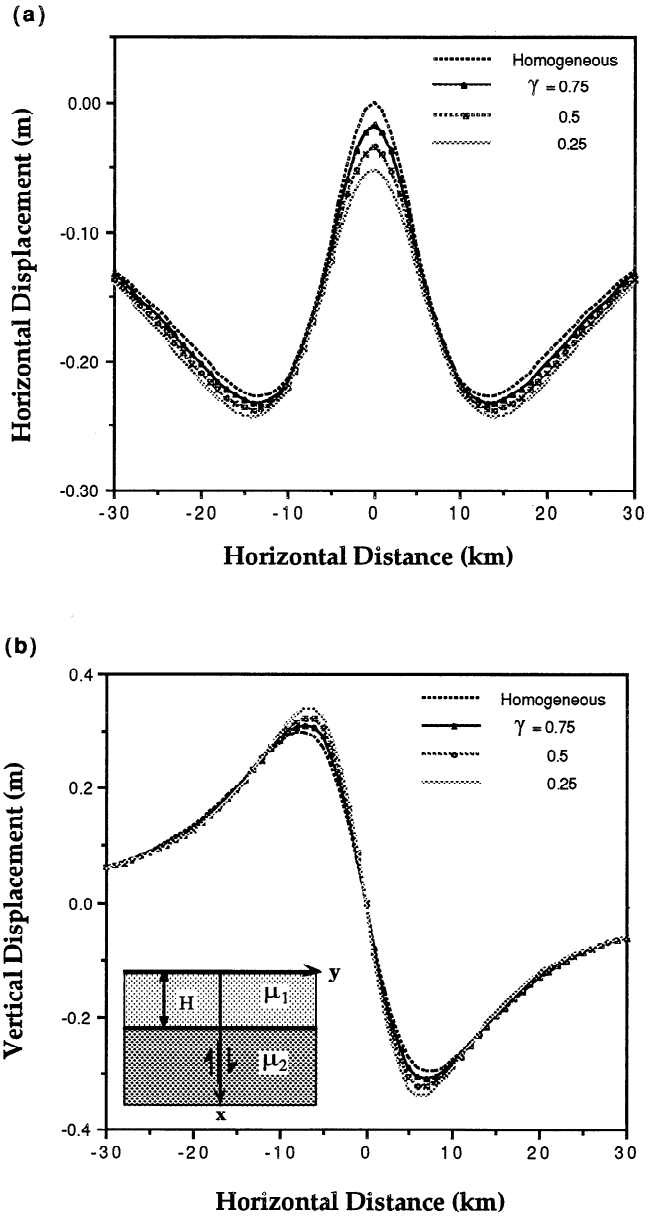

Figure 8. First-order surface (a) horizontal and (b) vertical displacements due to a vertical edge dislocation in a horizontally layered semi-infinite medium as a function of horizontal distance for $\gamma = \mu_1/\mu_2 = 0.25$, 0.5, and 0.75. The thickness of the surface layer is 5 km, and the top of the vertical edge dislocation is located at 9 km depth and has a length of 10 km. The amount of slip is prescribed as 2 m.

dislocation is located at 9-km depth and has a length of 10 km. The amount of reverse slip is prescribed as 2 m. The horizontal and vertical displacements at the free surface for $\gamma = 0.75$, 0.5, and 0.25 are shown in Figures 8a and 8b, respectively. It is shown that the vertical and horizontal displacements are amplified due to the softer surface layer. When the distance from the dislocation source increases, the influence of the soft surface layer decreases, and the first-order solution merges with the solution for a homogeneous half-plane as expected. The effect of layering is more pronounced for a more compliant surface layer.

A Horizontal Edge Dislocation in a Semi-infinite Medium With a Vertical Boundary

As a second example, we consider a horizontal edge dislocation in a semi-infinite medium with a vertical boundary (Figure 9 insert). The distance between the left tip of the edge dislocation and the layer interface is 1.5 km. The dislocation is located at a depth of 9 km and has a length of 8 km with the center at $y = 0$. Figures 9a and 9b show the horizontal and vertical displacements, respectively, for $\gamma = 0.25$ and the amount of slip of 2 m. The horizontal displacements are reduced significantly due to the presence of the stiffer material. As expected, the stiffer material reduces vertical displacements significantly on the left ($y < 0$). On the other hand, the peak uplift on the right side ($y > 0$) is slightly amplified. This amplification reduces rapidly to zero, and the solution merges with that for a homogeneous half-plane as the observation point moves away from the material boundary.

Dislocation Models for the 1989 Kalapana Earthquake

One of the unresolved issues from the initial studies of the *M*6.1 1989 Kalapana, Hawaii, earthquake is the discrepancy between the geodetically inferred location of the fault plane and that inferred from seismic data. *Arnadottir et al.* [1991] analyzed vertical displacements determined by repeated leveling. They found that the data could be well fit by a flat-lying dislocation with uniform slip at a depth of 4 ± 1 km (Figure 10). However, the focal depth of the earthquake determined from a local short period network is 9 km, 5 km deeper than imaged by the geodetic inversion. *Arnadottir et al.* [1991] noted that shallow basalt flows have low seismic velocities [*Klein*, 1981], and they suggested that a compliant surface layer overlaying stiffer rocks would bias the geodetically determined depth. Using a finite element method, they found that a compliant surface layer concentrates deformation, causing the dislocation modeled in a homogeneous half-space to be shallower than it really is. They suggested that the effect of a shallow compliant zone could explain part of the discrepancy between the geodetic and seismic depths. There are also significant lateral variations in elastic properties on Kilauea. The core of the east rift zone, thought to be composed a dense solidified dike swarm, exhibits high densities and velocities [*Hill and Zucca*, 1987] and is likely to be less compliant than the flank next to it.

The first-order perturbation solution showing the effect of a compliant surface layer on the vertical displacement is illustrated in Figure 11. The thickness of the compliant surface layer (see Figure 11 insert for geometrical configuration of the problem) is 5 km. The fault is located at the hypocentral depth of 9 km with a length of 8 km. Both seismic and geodetic studies indicate that the fault plane is subhorizontal. *Arnadottir et al.* [1991] take the ratio of the shear modulus of the surface compliant layer to that of the stiffer substrate to be 0.34 based on seismic velocity and density models [*Hill and Zucca*, 1987; *Klein*, 1981]. Poisson's ratio is taken to be everywhere 0.25. The amount of the horizontal slip is specified as 2 m. The effect of the compliant layer is to increase the amplitude and slightly decrease the half-width of the vertical displacements. In a homogeneous body the half-width of the subsidence is controlled by the fault depth. Thus the effect of the compliant surface layer is to make the dislocation appear shallower than it really is.

To account for both vertical and lateral variations in stiffness, we superpose a layered model and a model with a stiff vertical strip representing the rift axis (Figure 12). The width of the stiff

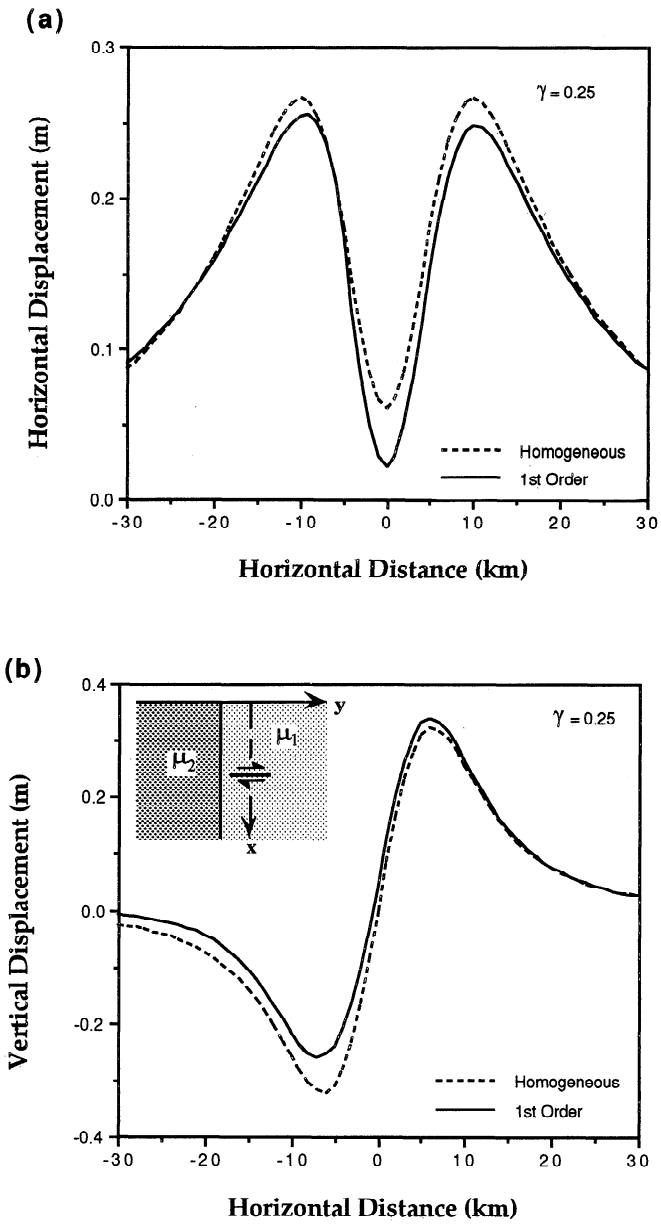

Figure 9. First-order surface (a) horizontal and (b) vertical displacements due to a horizontal edge dislocation in a vertically layered semi-infinite medium as a function of horizontal distance for $\gamma = \mu_1/\mu_2 = 0.25$. The horizontal edge dislocation is located at a depth of 9 km and has a length of 8 km. The amount of slip is prescribed as 2 m. The distance from the layer interface to the left tip of the horizontal edge dislocation is 1.5 km.

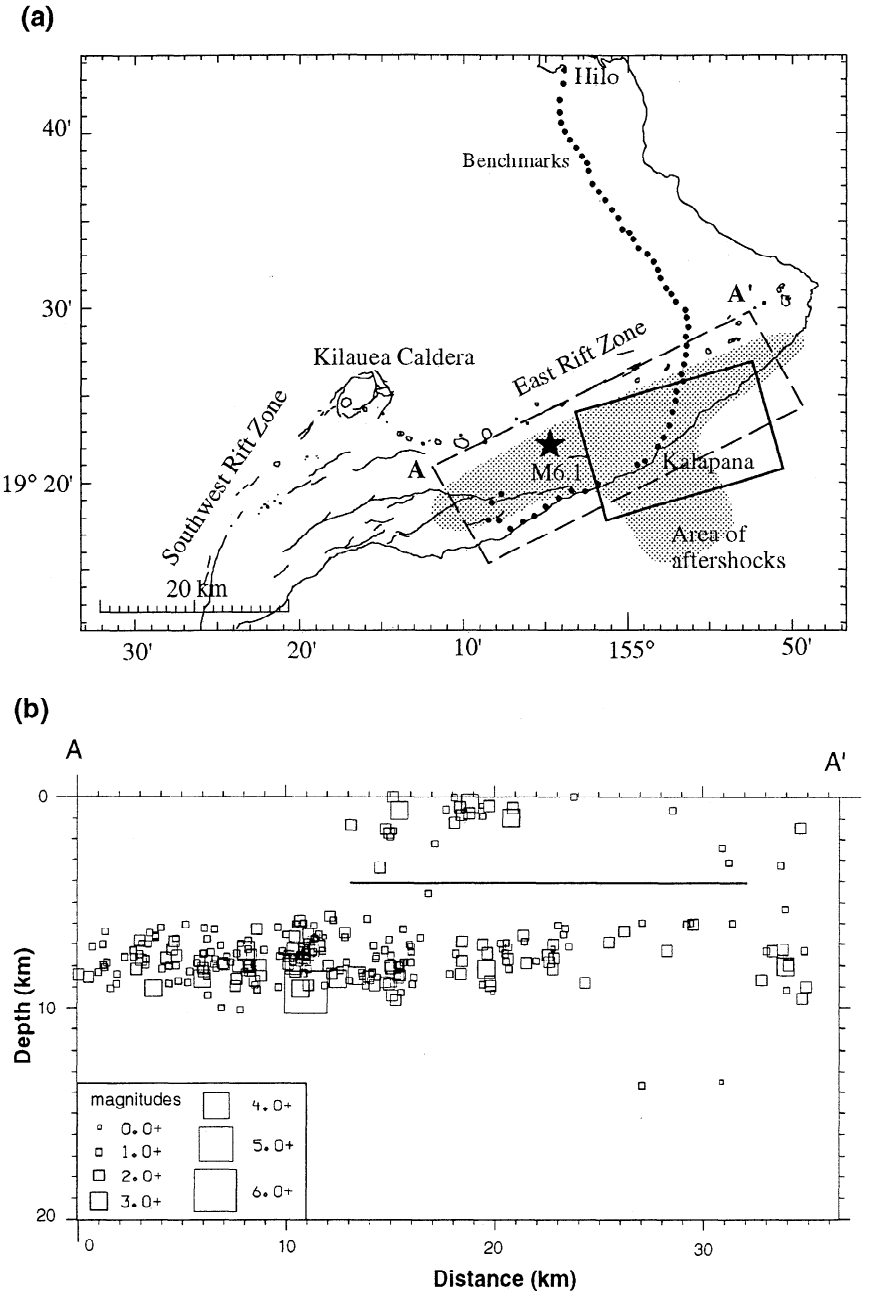

Figure 10. (a) Map of level line surveyed before and after the 1989 Kalapana, Hawaii earthquake. The location of the main shock epicenter is shown by a star, the aftershock zone by the shaded region, and the surface projection of the dislocation in a homogeneous medium that best fits the leveling data by the solid rectangle [*Arnadottir et al.*, 1991]. The dashed rectangle indicates the location of the cross section shown in Figure 10b. (b) Aftershocks of the 1989 Kalapana earthquake projected onto a vertical plane A - A'. The aftershocks cover a period from June 24, 1989 to September 1, 1989. The location of dislocation surface estimated from the inversion of geodetic data assuming a uniform half-space is shown by the solid line. Largest square is mainshock. (c) Coseismic elevation changes associated with the 1989 Kalapana earthquake (solid dots), as a function of distance along the leveling route. Calculated elevation changes predicted by a fault in a homogeneous half-space at a depth of 9 km dipping 4° NW are shown by the dashed curve. The prediction for a fault at 4 km depth, which best fits the leveling data, is shown as a solid curve. Data are after *Arnadottir et al.* [1991].

strip is 8 km, and the distance between right boundary of the strip to the left tip of the horizontal fault is 5.5 km. The fault is, as in the previous case, located at a depth of 9 km, with a length of 8 km and slip magnitude of 2 m. The vertical surface displacement for the inhomogeneous model is shown in Figure 13. For comparison, we also plot the vertical displacements due to faults at 5 km and 9 km depth in a homogeneous half-plane. The magnitude of the peak subsidence is scaled to be the same in the different models, since we do not know a priori the magnitude of the fault slip. Due to the inherently three-dimensional nature of

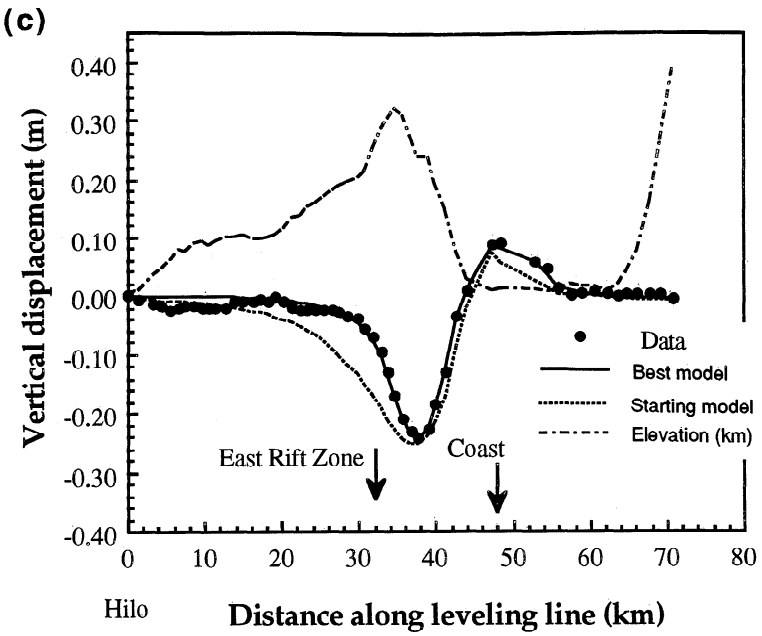

Figure 10. (continued)

the 1989 earthquake we cannot invert the data using a two-dimensional model. Rather, we use the two-dimensional results as a guide to the effects of elastic heterogeneity. In this sense, the vertical displacement profile produced by a fault at 9 km depth represents the expectation from the seismic data and that at 5 km in a homogeneous medium represents the geodetic model of *Arnadottir et al.* [1991].

We find that the effect of lateral heterogeneity is to narrow the zone of subsidence north of the dislocation (Figure 13). The net effect is to cause the dislocation to appear shallower than it really is. On the basis of the results shown in Figure 13 it appears that the current model explains about half of the discrepancy between the seismic and geodetic depth estimates. The inclusion of both vertical and horizontal variations in the elastic properties explains a larger part of the discrepancy than does layering alone. Note from Figure 10 that beyond a distance of 48 km the level line runs along the coastline, perpendicular to the inferred slip direction. Data from this part of the level line thus cannot be modeled with a two-dimensional calculation. A more complete comparison of the model and the data will be possible with three-dimensional Green's functions.

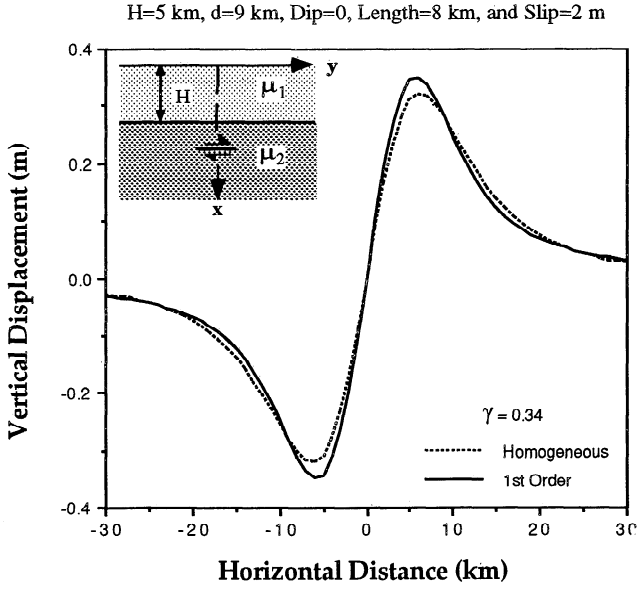

Figure 11. First-order surface vertical displacements due to a horizontal edge dislocation in a horizontally layered semi-infinite medium as a function of horizontal distance for $\gamma = \mu_1/\mu_2 = 0.34$. The thickness of the compliant surface layer is 5 km. Dislocation is located at the depth of 9 km with a length of 8 km and slip of 2 m.

Conclusions

We have investigated dislocations in inhomogeneous media using a moduli perturbation approach. A general formulation of the moduli perturbation procedure is presented, and a few solutions for anti- and in-plane problems in 2-D semi-infinite inhomogeneous media are obtained. It is found that first-order correction to the displacements can be represented by a volume integral in terms of the variations in moduli, the zero-order solution, and the displacement Green's function for the reference state. The same representation can be used to iterate for higher-order solutions. The volume integral can be reduced to a surface integral (or line integral in 2-D) if there are only piecewise constant variations in shear modulus. Comparisons with the available analytical solutions have indicated that the first-order perturbation solutions are valid over a wide range of variations in moduli. A simple two-dimensional model with the inclusion of both vertical and horizontal variations in the elastic properties can explain part of the discrepancy between seismic and geodetically inferred fault depths for the 1989 Kalapana, Hawaii, earthquake.

Although finite or boundary element methods can handle problems with inhomogeneities, the present perturbation approach has its advantages of simplicity, efficiency, and in some cases analytical forms of the results. The main limitation of the

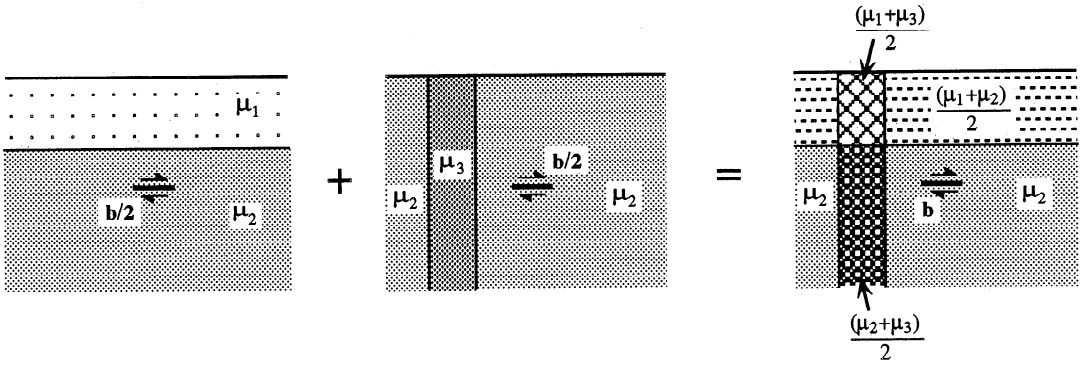

Figure 12. Superposition of a layered model and a stiffer vertical strip model to account for both vertical and horizontal variations of the material properties. Here, $\mu_1/\mu_2 = 0.34$, and $\mu_2/\mu_3 = 0.3$. Thus $[(\mu_1+\mu_2)/2]/\mu_2 = 0.67$, $[(\mu_1+\mu_3)/2]/\mu_2 = 1.84$, and $[(\mu_2+\mu_3)/2]/\mu_2 = 2.17$. The width of the stiff vertical strip is 8 km; the distance from right boundary of the stiff strip to the left tip of the horizontal fault is 5.5 km. The fault is at 9 km depth and has a length of 8 km and slip of 2 m.

perturbation method is that the variations in moduli should be modest so that δC_{ijkl} is small compared to $C^{(0)}_{ijkl}$ for the first-order solution to be accurate to the desired degree. While in theory one always can go to higher-order solutions for a better accuracy, only first-order solutions are easily obtainable for most practical problems. Perturbation solutions for dislocations in 3-D inhomogeneous media will be presented in a companion paper. The solutions will eventually be included in geodetic inversion algorithms for improved determination of fault geometry and spatially varying slip.

Appendix A: Perturbation Solutions for a Screw Dislocation in a Layered Semi-infinite Medium

A Screw Dislocation Buried in Substrate ($d \geq H$)

$$u_1^{(0)}(x_2, x_3) = \frac{b}{2\pi}\left[\tan^{-1}\left(\frac{x_2}{x_3+d}\right) - \tan^{-1}\left(\frac{x_2}{x_3-d}\right)\right] \tag{A1}$$

$$u_1^{(1)}(x_2, x_3) = \begin{cases} \dfrac{(1-\gamma)b}{4\pi}\left[\tan^{-1}\left(\dfrac{x_2}{d-x_3}\right) + \tan^{-1}\left(\dfrac{x_2}{d+x_3}\right)\right. \\ \left. - \tan^{-1}\left(\dfrac{x_2}{d+2H-x_3}\right) - \tan^{-1}\left(\dfrac{x_2}{d+2H+x_3}\right)\right] & x_3 \leq H \\ \dfrac{(1-\gamma)b}{4\pi}\left[\tan^{-1}\left(\dfrac{x_2}{d-2H+x_3}\right)\right. \\ \left. - \tan^{-1}\left(\dfrac{x_2}{d+2H+x_3}\right)\right] & x_3 \geq H \end{cases} \tag{A2}$$

$$u_1^{(2)}(x_2, x_3) = \begin{cases} \dfrac{(1-\gamma)^2 b}{8\pi}\left[\tan^{-1}\left(\dfrac{x_2}{d-x_3}\right) + \tan^{-1}\left(\dfrac{x_2}{d+x_3}\right)\right. \\ - 2\tan^{-1}\left(\dfrac{x_2}{d+2H-x_3}\right) - 2\tan^{-1}\left(\dfrac{x_2}{d+2H+x_3}\right) \\ \left. + \tan^{-1}\left(\dfrac{x_2}{d+4H-x_3}\right) + \tan^{-1}\left(\dfrac{x_2}{d+4H+x_3}\right)\right] & x_3 \leq H \\ \dfrac{(1-\gamma)^2 b}{8\pi}\left[\tan^{-1}\left(\dfrac{x_2}{d-2H+x_3}\right) - \tan^{-1}\left(\dfrac{x_2}{d+2H+x_3}\right)\right. \\ \left. + \tan^{-1}\left(\dfrac{x_2}{d+4H+x_3}\right) - \tan^{-1}\left(\dfrac{x_2}{d+x_3}\right)\right] & x_3 \geq H \end{cases} \tag{A3}$$

A Screw Dislocation in Surface Layer ($d \leq H$)

$$u_1^{(1)}(x_2, x_3) = \begin{cases} \dfrac{(1-\gamma)b}{4\pi}\left[\tan^{-1}\left(\dfrac{x_2}{d-2H+x_3}\right) + \tan^{-1}\left(\dfrac{x_2}{d+2H-x_3}\right)\right. \\ \left. + \tan^{-1}\left(\dfrac{x_2}{d-2H-x_3}\right) + \tan^{-1}\left(\dfrac{x_2}{d+2H+x_3}\right)\right] & x_3 \leq H \\ \dfrac{(1-\gamma)b}{4\pi}\left[\tan^{-1}\left(\dfrac{x_2}{d-x_3}\right) + \tan^{-1}\left(\dfrac{x_2}{d+x_3}\right)\right. \\ \left. + \tan^{-1}\left(\dfrac{x_2}{d-2H-x_3}\right) + \tan^{-1}\left(\dfrac{x_2}{d+2H+x_3}\right)\right] & x_3 \geq H \end{cases} \tag{A4}$$

$$u_1^{(2)}(x_2, x_3) = \begin{cases} -\dfrac{(1-\gamma)^2 b}{8\pi}\left[\tan^{-1}\left(\dfrac{x_2}{d+2H-x_3}\right) + \tan^{-1}\left(\dfrac{x_2}{d+2H+x_3}\right)\right. \\ + \tan^{-1}\left(\dfrac{x_2}{d-2H+x_3}\right) + \tan^{-1}\left(\dfrac{x_2}{d-2H-x_3}\right) \\ - \tan^{-1}\left(\dfrac{x_2}{d-4H+x_3}\right) - \tan^{-1}\left(\dfrac{x_2}{d-4H-x_3}\right) \\ \left. - \tan^{-1}\left(\dfrac{x_2}{d+4H-x_3}\right) - \tan^{-1}\left(\dfrac{x_2}{d+4H+x_3}\right)\right] & x_3 \leq H \\ -\dfrac{(1-\gamma)^2 b}{8\pi}\left[\tan^{-1}\left(\dfrac{x_2}{d+x_3}\right) + \tan^{-1}\left(\dfrac{x_2}{d-x_3}\right)\right. \\ \left. - \tan^{-1}\left(\dfrac{x_2}{d-4H-x_3}\right) - \tan^{-1}\left(\dfrac{x_2}{d+4H+x_3}\right)\right] & x_3 \geq H \end{cases} \tag{A5}$$

The solutions for a finite screw dislocation from d to D can be obtained by superposing a negative dislocation at depth D.

Appendix B: Displacement Green's Function for a Half-Plane

The displacement Green's functions for a half-plane corresponding to point forces have been given by *Maruyama* [1966], or they can be derived from Airy stress functions given by *Melan* [1932]. Using the familiar relationship between elastic constants in plane stress and plane strain, Melan's plane stress results can be transformed to the corresponding plane strain solution. For a force per unit length $F^{\perp}$ perpendicular to the free surface located

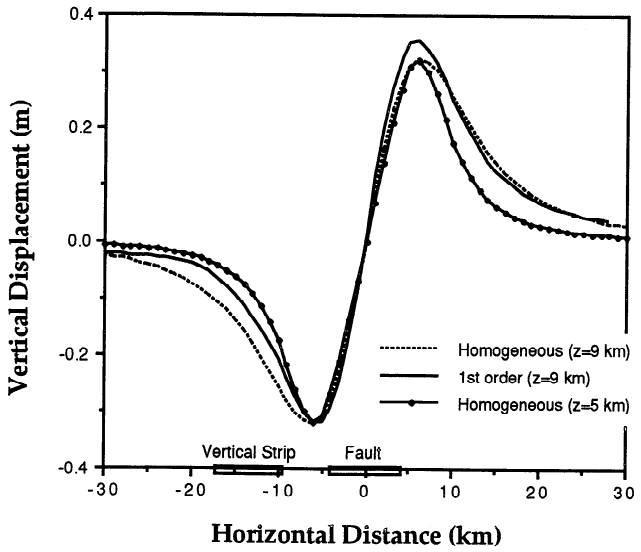

Figure 13. Comparison of vertical displacements due to faults at 5 km and 9 km depth in a homogeneous elastic half-plane with those due to a fault at 9 km depth in a inhomogeneous half-plane with both vertical and lateral variations in shear modulus shown in Figure 12.

at $(x = \zeta, y = \xi)$, the appropriate Airy stress function $\phi^{\perp}$ is

$$\phi^{\perp} = \frac{F^{\perp}}{\pi}\left\{\frac{(y-\xi)(\theta_1+\theta_2)}{2} - \frac{1}{2(1-\nu)}\left[\frac{\zeta x(\zeta+x)}{r_1^2} + \frac{(1-2\nu)}{2}(x-\zeta)\ln\frac{r_1}{r_2}\right]\right\} \tag{B1}$$

where

$$\begin{aligned} r_1^2 &= (x-\zeta)^2 + (y-\xi)^2 \\ r_2^2 &= (x+\zeta)^2 + (y-\xi)^2 \\ \theta_1 &= \tan^{-1}[(y-\xi)/(x-\zeta)] \\ \theta_2 &= \tan^{-1}[(y-\xi)/(x+\zeta)] \end{aligned} \tag{B2}$$

The Airy stress function for a force $F^{\parallel}$ parallel to the free surface, $\phi^{\parallel}$ is

$$\phi^{\parallel} = \frac{F^{\parallel}}{\pi}\left\{-(x-\zeta)\frac{(\theta_1+\theta_2)}{2} + \frac{1}{2(1-\nu)}\left[\frac{\zeta x(y-\xi)}{r_2^2} - \frac{(1-2\nu)}{2}(y-\xi)\ln\frac{r_1}{r_2}\right]\right\} \tag{B3}$$

The displacement Green's function can be obtained in a straightforward manner using *Mura*'s [1968] table. Since the displacement Green's functions were given in a different coordinate system in terms of the Lamé constant λ and shear modulus μ by *Maruyama* [1966], for the sake of convenience to the readers, we below give the expressions in the coordinate system used in this paper in terms of the shear modulus and Poisson's ratio.

$$G_{11} = -\frac{1}{2\pi\mu(1-\nu)}\left\{\frac{(3-4\nu)}{4}\ln r_1 + \frac{(8\nu^2-12\nu+5)}{4}\ln r_2 - \frac{(x-\zeta)^2}{4r_1^2} - \frac{(3-4\nu)(x+\zeta)^2 - 2\zeta(x+\zeta) + 2\zeta^2}{4r_2^2} - \frac{\zeta x(x+\zeta)^2}{r_2^4}\right\} \tag{B4}$$

$$G_{21} = \frac{1}{2\pi\mu(1-\nu)}\left\{(1-2\nu)(1-\nu)\theta_2 - \frac{(x-\zeta)(y-\xi)}{4r_1^2} - \frac{(3-4\nu)(x-\zeta)(y-\xi)}{4r_2^2} - \frac{\zeta x(x+\zeta)(y-\xi)}{r_2^4}\right\} \tag{B5}$$

$$G_{12} = \frac{1}{2\pi\mu(1-\nu)}\left\{-(1-2\nu)(1-\nu)\theta_2 - \frac{(x-\zeta)(y-\xi)}{4r_1^2} - \frac{(3-4\nu)(x-\zeta)(y-\xi)}{4r_2^2} + \frac{\zeta x(x+\zeta)(y-\xi)}{r_2^4}\right\} \tag{B6}$$

$$G_{22} = -\frac{1}{2\pi\mu(1-\nu)}\left\{\frac{(3-4\nu)}{4}\ln r_1 + \frac{(8\nu^2-12\nu+5)}{4}\ln r_2 + \frac{(x-\zeta)^2}{4r_1^2} + \frac{(3-4\nu)(x+\zeta)^2 + 2\zeta(x+\zeta) - 2\zeta^2}{4r_2^2} - \frac{\zeta x(x+\zeta)^2}{r_2^4}\right\} \tag{B7}$$

Appendix C: Stresses due to an Inclined Edge Dislocation in a Half-Plane

The stress field due to an edge dislocation in a plane strain semi-infinite medium has been given by *Head* [1953]. However, there is a misprint in his equation (13) for σ_{xx} when the Burger's vector is perpendicular to free surface. The corrected expressions will be given below.

For an inclined edge dislocation located at $(x = \zeta, y = \xi)$ making an angle α with the x axis (Figure C1), we have the x- and y-components of the Burger's vector b to be $b_x = b\cos\alpha$, and $b_y = b\sin\alpha$, respectively. The expressions for stresses according to *Head* [1953] are (with correction for his equation (13)):

$$\begin{aligned} \sigma_{11} = {} & \frac{\mu b_x}{2\pi(1-\nu)}\left\{\frac{(y-\xi)[3(x-\zeta)^2+(y-\xi)^2]}{[(x-\zeta)^2+(y-\xi)^2]^2} + \frac{(y-\xi)[3(x+\zeta)^2+(y-\xi)^2]}{[(x+\zeta)^2+(y-\xi)^2]^2}\right. \\ & + 4\zeta x(y-\xi)\frac{[3(x+\zeta)^2-(y-\xi)^2]}{[(x+\zeta)^2+(y-\xi)^2]^3}\Big\} \\ & + \frac{\mu b_y}{2\pi(1-\nu)}\left\{\frac{(x-\zeta)[(x-\zeta)^2-(y-\xi)^2]}{[(x-\zeta)^2+(y-\xi)^2]^2} - \frac{(x+\zeta)[(x+\zeta)^2-(y-\xi)^2]}{[(x+\zeta)^2+(y-\xi)^2]^2}\right. \\ & \left. + 2\zeta\frac{[(3x+\zeta)(x+\zeta)^3 - 6x(x+\zeta)(y-\xi)^2 - (y-\xi)^4]}{[(x+\zeta)^2+(y-\xi)^2]^3}\right\} \end{aligned} \tag{C1}$$

$$\begin{aligned} \sigma_{22} = {} & \frac{\mu b_x}{2\pi(1-\nu)}\left\{\frac{(y-\xi)[(x-\zeta)^2-(y-\xi)^2]}{[(x-\zeta)^2+(y-\xi)^2]^2} - \frac{(y-\xi)[(x+\zeta)^2-(y-\xi)^2]}{[(x+\zeta)^2+(y-\xi)^2]^2}\right. \\ & + 4\zeta(y-\xi)\frac{[(2\zeta-x)(x+\zeta)^2 + (3x+2\zeta)(y-\xi)^2]}{[(x+\zeta)^2+(y-\xi)^2]^3}\Big\} \\ & + \frac{\mu b_y}{2\pi(1-\nu)}\left\{\frac{(x-\zeta)[(x-\zeta)^2+3(y-\xi)^2]}{[(x-\zeta)^2+(y-\xi)^2]^2} - \frac{(x+\zeta)[(x+\zeta)^2+3(y-\xi)^2]}{[(x+\zeta)^2+(y-\xi)^2]^2}\right. \\ & \left. + 2\zeta\frac{[(x-\zeta)(x+\zeta)^3 - 6x(x+\zeta)(y-\xi)^2 + (y-\xi)^4]}{[(x+\zeta)^2+(y-\xi)^2]^3}\right\} \end{aligned} \tag{C2}$$

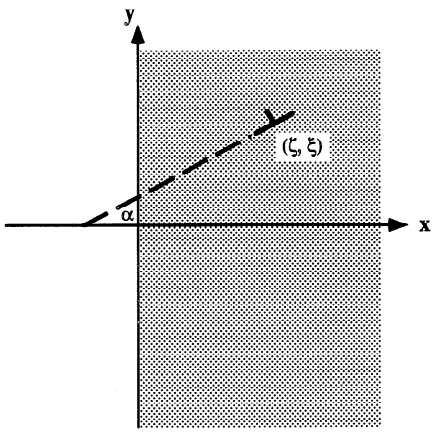

Figure C1. Geometrical configuration of an edge dislocation in a half-plane.

$$\sigma_{12}=\frac{\mu b_x}{2\pi(1-\nu)}\{\frac{(x-\zeta)[(x-\zeta)^2-(y-\xi)^2]}{[(x-\zeta)^2+(y-\xi)^2]^2}-\frac{(x+\zeta)[(x+\zeta)^2-(y-\xi)^2]}{[(x+\zeta)^2+(y-\xi)^2]^2}$$

$$+2\zeta\frac{[(\zeta-x)(x+\zeta)^3+6x(x+\zeta)(y-\xi)^2-(y-\xi)^4]}{[(x+\zeta)^2+(y-\xi)^2]^3}\}$$

$$+\frac{\mu b_y}{2\pi(1-\nu)}\{\frac{(y-\xi)[(x-\zeta)^2-(y-\xi)^2]}{[(x-\zeta)^2+(y-\xi)^2]^2}-\frac{(y-\xi)[(x+\zeta)^2-(y-\xi)^2]}{[(x+\zeta)^2+(y-\xi)^2]^2}$$

$$+4\zeta x(y-\xi)\frac{[3(x+\zeta)^2-(y-\xi)^2]}{[(x+\zeta)^2+(y-\xi)^2]^3}\} \quad \text{(C3)}$$

Appendix D: Displacements due to an Edge Dislocation in a Homogeneous Half-Plane

Displacements due to an edge dislocation in a homogeneous half-plane can be derived from *Mura* [1968]. We are particularly interested in the displacements at free surface giving below (see Figure C1 for geometry):

$$u_x=-\frac{1}{\pi}[b_x\tan^{-1}(\delta)+\frac{b_y+b_x\delta}{1+\delta^2}] \quad \text{(D1)}$$

$$u_y=-\frac{1}{\pi}[b_y\tan^{-1}(\delta)+\frac{b_x-b_y\delta}{1+\delta^2}] \quad \text{(D2)}$$

where $\delta=(y-\xi)/\zeta$.

Acknowledgments. This research was funded by the NSF grant EAR-9218556. We thank Allan Rubin, Joan Gomberg, and Guust Nolet for their critical reviews of the manuscript.

References

Aki, K., and P. Richards, *Quantitative Seismology: Theory and Methods*, vol. 2, W. H. Freeman, New York, 1980.

Arnadottir, T., and P. Segall, The 1989 Loma Prieta earthquake imaged from inversion of geodetic data, *J. Geophys. Res.*, in press, 1994.

Arnadottir, T., P. Segall, and P. T. Delaney, A fault model for the 1989 Kilauea south flank earthquake from leveling and seismic data, *Geophys. Res. Lett., 18*, 2217-2220, 1991.

Arnadottir, T., P. Segall, and M. Matthews, Resolving the discrepancy between geodetic and seismic fault models for the 1989 Loma Prieta, California, earthquake, *Bull. Seismol. Soc. Am., 82*, 2248-2255, 1992.

Barnett, D. M., On the screw dislocation in an inhomogeneous elastic medium: The case of continuously varying elastic moduli, *Int. J. Solids Struct., 8*, 651-660, 1972.

Bender, C. M., and S. A. Orszag, *Advanced Mathematical Methods for Sciences and Engineers*, McGraw-Hill, New York, 1978.

Chinnery, M. A., The deformation of the ground around surface faults, *Bull. Seismol. Soc. Am., 51*, 355-372, 1961.

Du, Y., A. Aydin, and P. Segall, Comparison of various inversion techniques as applied to the determination of a geophysical deformation model for the 1983 Borah Peak earthquake, *Bull. Seismol. Soc. Am.*, *82*, 1840-1866, 1992.

Eberhart-Phillips, D., and W. D. Stuart, Material heterogeneity simplifies the picture: Loma Prieta, *Bull. Seismol. Soc. Am., 82*, 1964-1968, 1992.

Fan, H., L. M. Keer, and T. Mura, Inhomogeneity problem revisited via the modulus perturbation approach, *Int. J. Solids Struct., 29*, 2583-2594, 1992.

Gao, H., Fracture analysis of nonhomogeneous materials via a moduli-perturbation approach, *Int. J. Solids Struct., 27*, 1663-1682, 1991.

Gao, H., C.-H. Chiu, and J. Lee, Elastic contact versus indentation modeling of multi-layered materials, *Int. J. Solids Struct., 29*, 2471-2492, 1992.

Head, A. K., Edge dislocations in inhomogeneous media, *Proc. Phys. Soc.*, *B66*, 793-801, 1953.

Hill, D. P., and J. J. Zucca, Geophysical constraints on the structure of Kilauea and Mauna Loa volcanoes and some implications for seismomagmatic processes, in Volcanism in Hawaii, edited by R.W. Decker, T.L. Wright, and P.H. Stauffer, *U.S. Geol. Surv. Prof. Pap. 1350*, 903-917, 1987.

Hudson, J. A., and J. R. Heritage, The use of the Born approximation in seismic scattering problems, *Geophys. J. R. Astron. Soc., 66*, 221-240, 1981.

Klein, F.W., A linear-gradient crustal model for south Hawaii, *Bull. Seismol. Soc. Am., 71*, 1503-1510, 1981.

Lee, M.-S., and J. Dundurs, Edge dislocation in a surface layer, *Int. J. Eng. Sci., 11*, 87-94, 1973.

Lisowski, M., W. H. Prescott, J. C. Savage, and M. J. Johnston, Geodetic estimate of coseismic slip during the 1989 Loma Prieta, California, earthquake, *Geophys. Res. Lett., 17*, 1437-1440, 1990.

Mahrer, K. D., and A. Nur, Strike slip faulting in a downward varying crust, *J. Geophys. Res., 84*, 2296-2302, 1979.

Marshall, G. A., R. Stein, and W. Thatcher, Faulting geometry and slip from co-seismic elevation changes: The 18 October 1989, Loma Prieta, California, earthquake, *Bull. Seismol. Soc. Am., 81*, 1660-1693.

Maruyama, T., On two-dimensional elastic dislocations in an infinite and semi-infinite medium, *Bull. Earthquake Res. Inst. Univ. Tokyo, 44*, 811-871, 1966.

Meertens, C. M., and J. M. Wahr, Topographic effect on tilt, strain, and displacement measurements, *J. Geophys. Res., 91*, 14,057-14,062, 1986.

McTigue, D. F., and P. Segall, Displacements and tilts from dip-slip faults and magma chambers beneath irregular surface topography, *Geophys. Res. Lett., 15*, 601-604, 1988.

McTigue, D. F., and R. S. Stein, Topographic amplication of tectonic displacement: Implications for geodetic measurement of strain changes, *J. Geophys. Res., 89*, 1123-1131, 1984.

Melan, E., Der spannungszustand der durch eine eingelkraft im innern beanspruchten halbscheibe, *Angew. Math. Mech., 12*, 343-346, 1932. (Correction, *Z. Angew. Math. Mech., 20*, 368, 1940.)

Mura, T., The continuum theory of dislocations, in *Advances in Materials Research*, vol. 3, edited by H. Herman, pp.1-108, John Wiley, New York, 1968.

Muskhelishvilli, N. I., *Some Basic Problems of the Mathematical Theory of Elasticity*, Noordhoff, Leiden, Netherlands, 1953.

Press, W. H., B. P. Flannery, S. A. Teukolsky, and W. T. Vetterling, *Numerical Recipes*, Cambridge University Press, New York, 1986.

Roth, F., Subsurface deformations in a layered elastic half-space, *Geophys. J. Int., 103*, 147-155, 1990.

Rybicki, K., The elastic residual field of a very long strike-slip fault in the presence of a discontinuity, *Bull. Seismol. Soc. Am., 61*, 79-92, 1971.

Rybicki, K., and K. Kasahara, A strike-slip fault in a laterally inhomogeneous medium, *Tectonophysics, 42*, 127-138, 1977.

Savage, J. C., Effect of crustal layering on dislocation modeling, *J. Geophys. Res., 92*, 10,595-10,600, 1987.

Segall, P., and R. Harris, Slip deficit on the San Andreas fault at Parkfield, California, as revealed by inversion of geodetic data, *Science, 233*, 1409-1413, 1986.

Steketee, J. A., Some geophysical applications of the elasticity theory of dislocation, *Can. J. Phys., 36*, 1168-1197, 1958.

Walpole, L. J., The elastic field of an inclusion in an anisotropic medium, *Proc. R. Soc. London, Ser. A, 300*, 270-288, 1967.

Ward, S. N., and S. Barrientos, An inversion for slip distribution and fault shape from geodetic observations of the 1983, Borah Peak, Idaho, earthquake, *J. Geophys. Res., 91*, 4909-4919, 1986.

Weeks, R., J. Dundurs, and M. Stippes, Exact analysis of an edge dislocation near a surface layer, *Int. J. Eng. Sci., 6*, 365-372, 1968.

Y. Du, Department of Geological and Environmental Sciences, Stanford University, Stanford, CA, 94305. (e-mail: yijun@pangea.stanford.edu)

H. Gao, Division of Applied Mechanics, Stanford University, Stanford, CA 94305. (e-mail: gao@am-sun2.stanford.edu)

P. Segall, Department of Geophysics, Stanford University, Stanford, CA 94305. (e-mail: segall@kilauea.stanford.edu)

(Received July 19, 1993; revised January 24, 1994;
accepted January 31, 1994.)